Journal of Medicinal Chemistry

Article

pubs.acs.org/jmc

Lactam-Stapled Cell-Penetrating Peptides: Cell Uptake and Membrane Binding Properties

Marco J. Klein,[†] Samuel Schmidt,[§] Parvesh Wadhwani,[†] Jochen Bürck,[†] Johannes Reichert,[†] Sergii Afonin,[†] Marina Berditsch,[‡] Tim Schober,[‡] Roland Brock,[§] Manfred Kansy,[∥] and Anne S. Ulrich*[,†,‡]

[†]Institute of Biological Interfaces, Karlsruhe Institute of Technology, POB 3640, 76021 Karlsruhe, Germany

[‡]Institute of Organic Chemistry, Karlsruhe Institute of Technology, Fritz-Haber-Weg 6, 76131 Karlsruhe, Germany

[§]Department of Biochemistry, Radboud Institute for Molecular Life Sciences, Radboud University Medical Center, Geert Grooteplein 28, 6525 GA Nijmegen, The Netherlands

[∥]Roche Pharma Research and Early Development, Pharmaceutical Sciences, Roche Innovation Center Basel, F. Hoffmann-La Roche AG, Grenzacherstrasse 124, CH-4070 Basel, Switzerland

Supporting Information

ABSTRACT: Stapling of side chains to stabilize an α-helical structure has been generally associated with an increased uptake of CPPs. Here, we compare four amphiphilic stapled peptides with their linear counterparts in terms of their membrane binding and conformational features in order to correlate these with uptake efficiency and toxicological effects. The impact of lactam stapling was found to vary strongly with regard to the different aspects of peptide–membrane interactions. Nearly all stapled peptides caused less membrane perturbation (vesicle leakage, hemolysis, bacterial lysis) than their linear counterparts. In one case (MAP-1) where stapling enhanced α-helicity in aqueous and lipid environments, leakage was eliminated while cell uptake in HEK293 and HeLa cells remained high, which improved the overall characteristics. The other systems (DRIM, WWSP, KFGF) did not improve, however. The data suggest that cell uptake of amphipathic CPPs correlates with their adopted α-helix content in membranes rather than their helicity in solution.

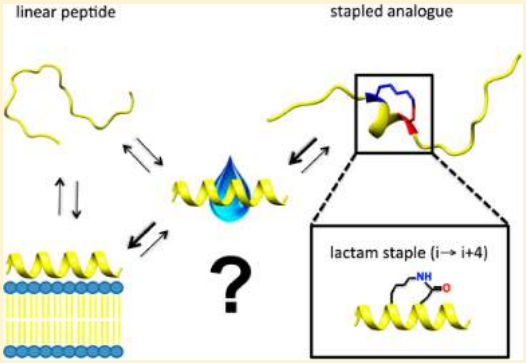

INTRODUCTION

Cell-penetrating peptides (CPPs) are peptides of typically 8–30 amino acids in length, which possess the ability to induce cellular uptake of themselves together with associated cargo.[1−3] In 1997, the first nucleic acids were delivered in vitro by a designer-made CPP, and cellular delivery was also established for proteins and peptides.[4,5] To date, a wealth of studies have been conducted on diverse CPPs for transporting covalently coupled or noncovalently associated cargo of various kinds, such as peptides, antibodies, nucleic acids, nanoparticles, and small molecule drugs.[2] Even though CPPs are promising tools to reach intracellular targets, no CPP-based drug has yet been approved. The use of biomacromolecules is still largely restricted to extracellular targets, while intracellular delivery remains a major challenge. Medical applications of CPPs are hampered by a poor understanding of the internalization process, insufficient cytoplasmic delivery upon endosomal capture, and low bioavailability and selectivity in living organisms.

Uptake of a CPP may occur by endocytosis[6,7] and/or by direct membrane permeation. A strong dependence has been reported on the type of peptide, its concentration, temperature, and the particular cargo, as well as on the cell line and lipid composition. For direct permeation, different translocation mechanisms across the plasma membrane via transient structures (inverted micelles, pores) or local rupture (carpet, membrane thinning) are being discussed.[8−11] When interacting with a cell membrane, such CPPs usually take on an amphipathic structure, while they are usually unstructured in aqueous solution, as is typical for short peptides. The folding of an initially disordered peptide on the membrane surface can lead to a massive destabilization of the lipid bilayer.[12−14] Especially in the case of helical CPPs with a secondary amphipathic profile, the formation and stability of this helix seem to be important for their delivery.

Helical secondary structure can be chemically stabilized by side-chain "stapling".[15] One means to achieve such staple is via formation of a lactam bridge between Lys and Glu/Asp residues.[16] Using this approach, Fairlie and co-workers designed single-turn α-helical peptides,[17] which reached 100% helicity according to circular dichroism and NMR analysis. Even when treated with 8 M guanidinium chloride, the most stable pentapeptide retained its α-helical conformation. Addi-

Received: June 7, 2017
Published: September 18, 2017

DOI: 10.1021/acs.jmedchem.7b00813
J. Med. Chem. 2017, 60, 8071−8082

tionally, this peptide showed enhanced stability against trypsinolysis compared to its linear analogue.

Studies addressing the functional effect of stapling on the cell-penetration ability of peptides are rare. The most comprehensive studies have been presented for peptides stabilized via hydrocarbon staples. Verdine et al. showed that cell penetration is strongly related to the formal charge (due to electrostatic attraction of the peptide to the cell surface) and to the position and type of the staple ($i \rightarrow i + 4$ staple, $i \rightarrow i + 7$ staple, $i \rightarrow i + 4 \rightarrow i + 11$ stitch).[18] For penetratin and octaarginine but not for TAT, hydrocarbon stapling improved their cell uptake. Another study focused on the position-dependent influence of the highly hydrophobic hydrocarbon staple and noted a nonlinear correlation of the uptake efficiency with the increase in hydrophobicity and helicity. At the same time, an improvement in uptake also showed some correlation with cytotoxicity.[19] The actual role of the staple in promoting uptake was, however, questioned by demonstrating that the improved time-dependent accumulation of a stapled peptide could be largely attributed to proteolytic stabilization and enhanced target binding.[20] Recently, Schmidt et al. incorporated a more polar lactam bridge in various patterns into highly hydrophobic nonpolar peptides and found that this cyclization enhanced the uptake only in some cases, after long-term incubation. Overall, in this study the linear peptides tended to be the most active,[21] though it has to be noted that the peptide selection did not contain any amphipathic CPPs.

To our knowledge, despite the general assumption of enhanced cell uptake due to α-helix stapling, no improvement has been ever reported for lactam bridges. For amphipathic CPPs, the question thus remains open whether they would benefit from lactam stapling, given that their intrinsic amphiphilic conformation seems to be the most important aspect in membrane perturbation.[22] We thus decided to examine several different lactam-stapled CPPs and their linear counterparts because lactam linkers confer the greatest and most ideal α-helicity compared to hydrocarbon or triazole linkers.[23] Furthermore, the present study is timely, as there are hardly any reports on lactam-stapled cell-penetrating peptides that describe their cell uptake behavior, even though this type of stapling is the oldest and best known.[15] The lactam bridge might be expected to allow the peptides to overcome the hydrophobic barrier of the membrane more efficiently if it stabilizes the amphiphilic structure. Therefore, our aim was to analyze the conformational features and membrane binding properties of four representative lactam-stapled CPPs and their linear counterparts and to determine their uptake efficiency into lipid vesicles and their interaction with various types of living cells. To obtain further insight into the translocation mechanism, we looked for correlations between structural stabilization and membrane binding on the one hand and cell translocation efficiency as well as membrane disruptive effects on the other hand.

RESULTS

Peptides. To assess the impact of backbone stapling, we chose four CPPs from different peptide classes. Our objective was always to directly compare the properties of the linear CPP and its constrained counterpart.

The well-known membranolytic peptide melittin from the venom of *Apis mellifera* is a prototypic membrane-active agent whose structural behavior and lipid interactions have been thoroughly investigated. Despite its high hemolytic side effects, it was shown to efficiently deliver DNA to the cytosol of eukaryotic cells, possibly by enhancing endosomal escape.[24] Both melittin and its amidated all-D-retro-inverso analogue **1** (DRIM) (QQRKRKIWSILAPLGTTLVKLVAGIG-NH_2)[25] contain at opposite ends one region that is predominantly hydrophobic and one region that is hydrophilic, and they tend to form an α-helix when bound to a lipid bilayer (Figures 1 and 2). Hence, due to their primary amphipathic character, these peptides can efficiently perturb cellular membranes.[26] The side chains of the D-retro-inverso analogue are superimposable with those of the original peptide, even though the N- and C-termini are on opposite sides and the helix is right-handed instead of left-handed. **1** is more resistant to biodegradation because of the D-amino acids.

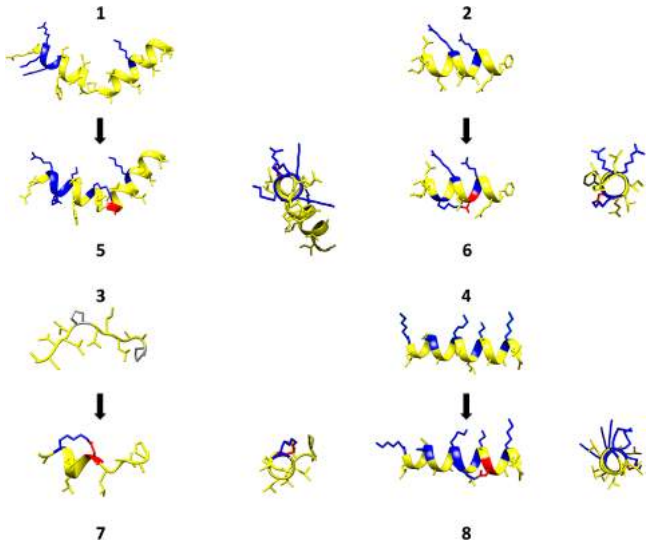

Figure 1. Models of the four linear CPPs **1**, **2**, **3**, and **4** (upper) and their stapled analogues **5**, **6**, **7**, and **8** (lower). Cationic amino acids are shown in blue, anionic ones in red, and the lactam bridge between Lys and Asp is in blue/red. Lower right: Views down the helix axis from N- to C-terminus.

In a remarkable screening approach by Wimley et al., a library of 24 000 randomly selected sequences revealed 18 peptides with a largely hydrophobic character that could spontaneously translocate across phospholipid bilayers and were also taken up by living cells.[27] By design, all these peptides shared a common motif, i.e., PLIL-XXXXX-GQF, PLIY-XXXXX-GQF, or XXXX-LRLLR-GQF (the GQF linker was used to attach and cleave a fluorophore). Due to their uptake via direct membrane translocation, they promised to be highly advantageous as they alleviate the risk of endosomal entrapment and degradation. We thus selected the short peptide **2** (WWSP) (PLILLRLLRGQF-NH_2), which had the highest uptake efficiency and capability for direct membrane crossing in CHO cells (Figures 1 and 2),[27] a capacity that was independently confirmed also in HEK and HeLa cells.[21]

Proteins that are destined for transport across cellular membranes are expressed as precursors with special N-terminal signal peptides. CPPs had been designed by conjugating such signal peptides to cationic nuclear localization sequences (NLS), e.g., by combining the hydrophobic region of the Kaposi fibroblast growth factor (KFGF) signal peptide with the NLS from the transcription factor NF-κB p50.[28] Our third peptide **3** (KFGF) (AAVLLPVLLAAP-NH_2) originates from

DOI: 10.1021/acs.jmedchem.7b00813
J. Med. Chem. 2017, 60, 8071−8082

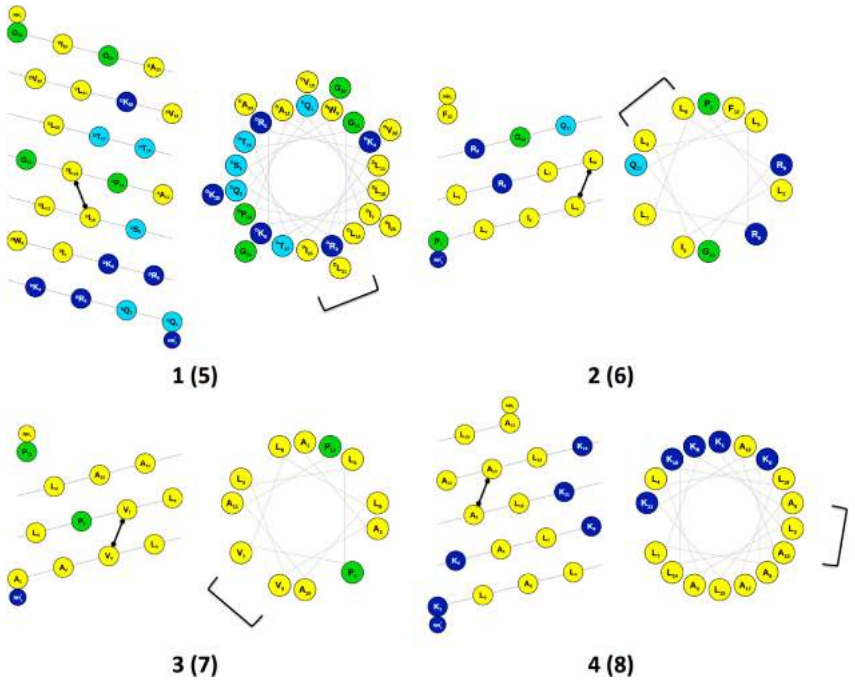

Figure 2. Helical net projections (left) and helical wheel plots (right) of the four CPPs **1**, **2**, **3**, and **4** drawn as ideal α-helices. The figures still contain the original amino acids to be replaced by the staple (Lys and Asp, from N- to C-terminus), which is illustrated by the connecting line. Cationic amino acids are shown in blue, polar amino acids in light blue, and glycine and proline are in green (graphics created with "Protein ORIGAMI" by KIT Karlsruhe, http://www.ibg.kit.edu/protein_origami/).

Table 1. Physicochemical Properties of the Designed Peptides[a]

peptide	CN	sequence	*L*	NC	PR/*n*%	NPR/%
DRIM	**1**	QQRKRKIWSILAPLGTTLVKLVAGIG-NH_2	26	+6	13/50.0	13/50.0
WWSP	**2**	PLILLRLLRGQF-NH_2	12	+3	4/33.3	8/66.7
KFGF	**3**	AAVLLPVLLAAP-NH_2	12	+1	0/0.0	12/100.0
MAP-1	**4**	KLALKALKALKAALKLA-NH_2	17	+6	5/29.4	12/70.6
sDRIM	**5**	QQRKRKIWS**K**LAP**D**GTTLVKLVAGIG-NH_2	26	+6	13/50.0	13/50.0
sWWSP	**6**	PLI**K**LRL**D**RGQF-NH_2	12	+3	4/33.3	8/66.7
sKFGF	**7**	AA**K**LLP**D**LLAAP-NH_2	12	+1	0/0.0	12/100.0
sMAP-1	**8**	KLALKALK**K**LKA**D**LKLA-NH_2	17	+6	5/29.4	12/70.6

[a]CN, compound number; *L*, length; NC, net charge; PR, number of polar residues; NPR, number of nonpolar residues. Prefix "s" is added to the stapled counterparts, i.e., sDRIM, sWWSP, sKFGF, and sMAP-1. The bold and underlined lysine (K) and aspartic acid (D) indicate the position of the lactam staple.

this sequence and is known to be able to translocate membranes per se (Figures 1 and 2).[28] It is the only peptide in our study without an amphipathic character, but we included it to study the effect of a lactam bridge using a signal sequence-based CPP representative.

Although most of the amphipathic CPPs possess a net positive charge, there is evidence that the actual uptake process is driven by the amphiphilicity per se and not just by electrostatic accumulation on the anionic cell surface. Studies with the "sweet arrow peptide" (SAP) and its all-Arg/all-Glu analogue SAP(E), a neutral and an anionic analogue of the model amphipathic peptide (MAP), had shown that as long as the amphipathic character of the peptide is maintained, its cell-penetrating capacity is also preserved.[22,29−31] Therefore, we incorporated a variant of MAP that had been rationally designed with a cationic secondary amphipathic character.[30] We named this C-terminally amidated analogue **4** (MAP-1) (KLALKALKALKAALKLA-NH_2).[32] Forming an ideal α-helix, it is a perfect candidate for stapling because of its repetitive sequence that should minimize the influence of the position of the lactam bridge (Figures 1 and 2). The sequences and physicochemical properties of the designed peptides are listed in Table 1.

Positioning of the Staple. The aim was to test whether helix stabilization via lactam stapling would improve the cell permeability in any of the four peptides, ideally without affecting their cytotoxic features. Especially in the case of **4** but also for **1** and **2**, one might expect that the formation and stability of the amphipathic α-helix would be a critical feature for function as a CPP.[23] The lactam bridge was implemented by exchanging two amino acids for Lys and Asp in an $i \rightarrow i + 4$ pattern. We located the most suitable positions for lactam-stapling according to the following considerations: in the cases of **2** and **4**, as recommended by Walensky et al.,[19] we positioned the staple at the interface between the hydrophilic and hydrophobic faces of the potential α-helix in order to not disturb the amphipathic character (Figure 2). In both **1** and **3**, we locked a helical turn that contains a proline, which is generally known as a helix breaker, in order to enhance the continual α-helical character (Figure 2). In all cases, only

DOI: 10.1021/acs.jmedchem.7b00813
J. Med. Chem. 2017, 60, 8071−8082

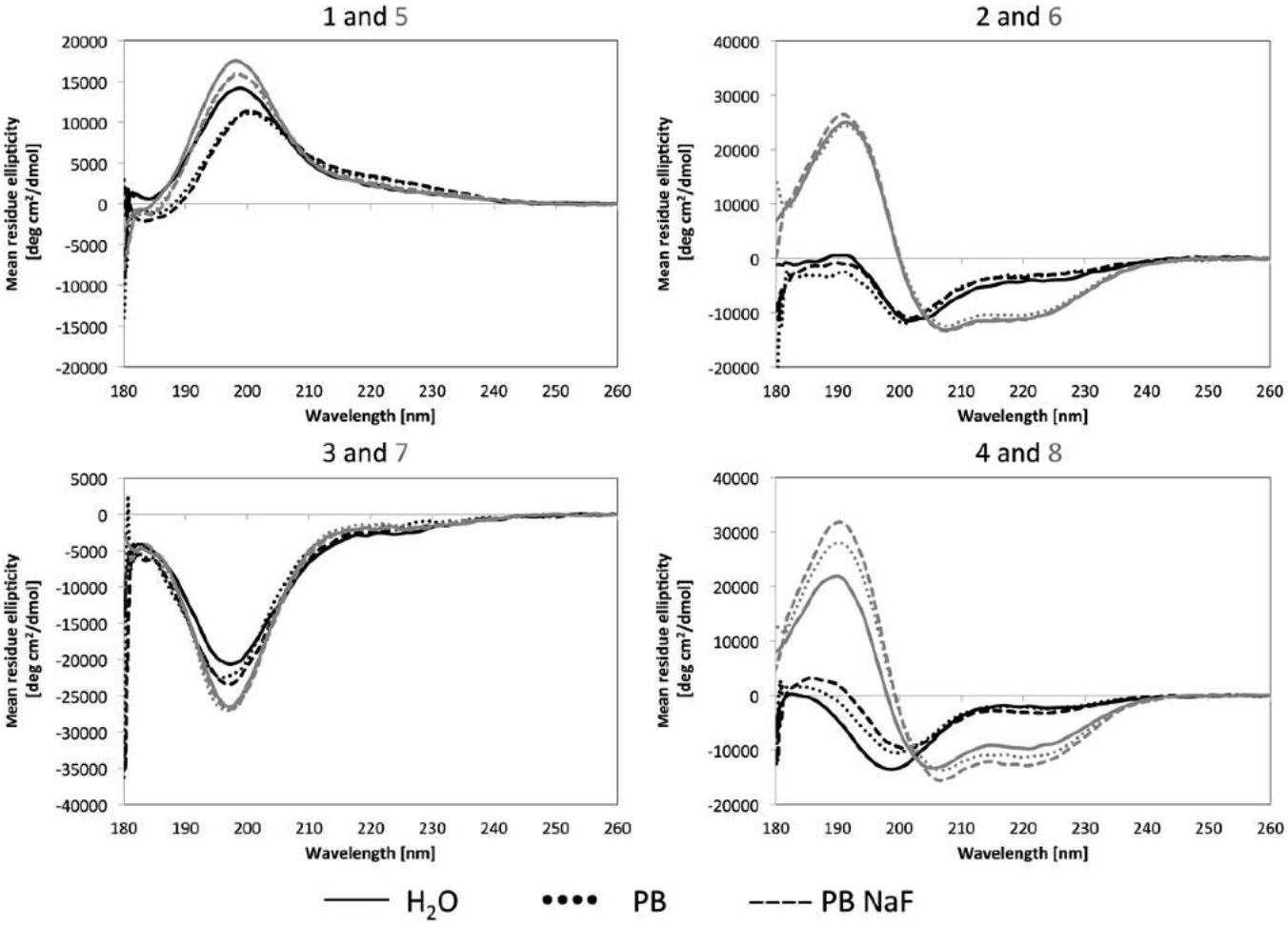

Figure 3. CD spectra in aqueous solutions [pure water (H_2O), phosphate buffer (PB, 10 mM), and phosphate buffer with high salt (NaF, 100 mM)] of the four linear CPPs **1**, **2**, **3**, and **4** and their stapled analogues **5**, **6**, **7**, and **8**. Spectra of the stapled analogues are displayed as gray lines. Note that all spectra of **1** and **5** are inverted, as expected for a peptide consisting of D-amino acids only.

uncharged amino acids were exchanged in order to maintain the overall net charge of the peptides.

Structural Characterization. All peptides were synthesized in the linear and stapled form for comparison of their biophysical and biological properties. First, we determined the impact of the lactam bridge on the α-helix content, using circular dichroism (CD) spectroscopy in three different conditions: pure water (H_2O), phosphate buffer (PB, 10 mM), and phosphate buffer containing additionally a high salt concentration (NaF, 100 mM). High ionic strength should help to stabilize the secondary structure of charged peptides due to charge screening.[33,34]

Our CD data show that all four linear peptides were generally disordered in aqueous solution, as expected, but prominent effects were seen regarding the impact of the staple. In the cases of **5** and **7** (Figure 3), stapling did not induce any conformational change, as these analogues remained just as unstructured. On the other hand, **6** and **8** (Figure 3) assumed an α-helical conformation in aqueous solution, in contrast to their unstructured linear counterparts. An impact of charge screening on the secondary structure could be observed for the stapled analogues **6** and **8**. Here, the presence of high salt led to more pronounced helices, especially for **8**.

Next, we analyzed the secondary structure of the CPPs in various membrane environments, using lipid vesicles of different composition. POPC was used to model a simple phospholipid bilayer, given that uncharged phosphatidylcholines are the most abundant lipids in eukaryotic plasma membranes. The introduction of anionic lipids in the mixture POPC/POPG (3/1) served mainly to enhance binding of the cationic peptides, but we note that anionic lipids are highly abundant in mitochondria and bacterial membranes. In the composition of POPC/lysoPC (9/1), the membranes were softened with lyso-lipid to enhance peptide penetration, while POPC/Chol (3/1) was used to make the membranes more rigid.[35] The α-helix content of each sample was estimated by deconvolution of the corresponding CD spectrum using the programs CONTIN and CDSSTR, which are provided by DICHROWEB online server.[36−41]

Interestingly, when studying the four peptides in a membrane environment, stapling did not enhance α-helix formation compared to any of the corresponding linear sequences. **1** (Figure 4) showed an average α-helix content of 50% [POPC 61%; POPC/POPG 40%; POPC/lysoPC 57%; POPC/Chol 43%]. Here, the influence of the membrane environment is obvious, as the same peptide had been completely unstructured in the aqueous solutions. The stapled analogue **5**, however, had a lower α-helix content of only 31% [POPC 26%; POPC/POPG 51%; POPC/lysoPC 23%; POPC/Chol 24%] (Figure 4). This lower value may be attributed to the fact that the

DOI: 10.1021/acs.jmedchem.7b00813
J. Med. Chem. 2017, 60, 8071−8082

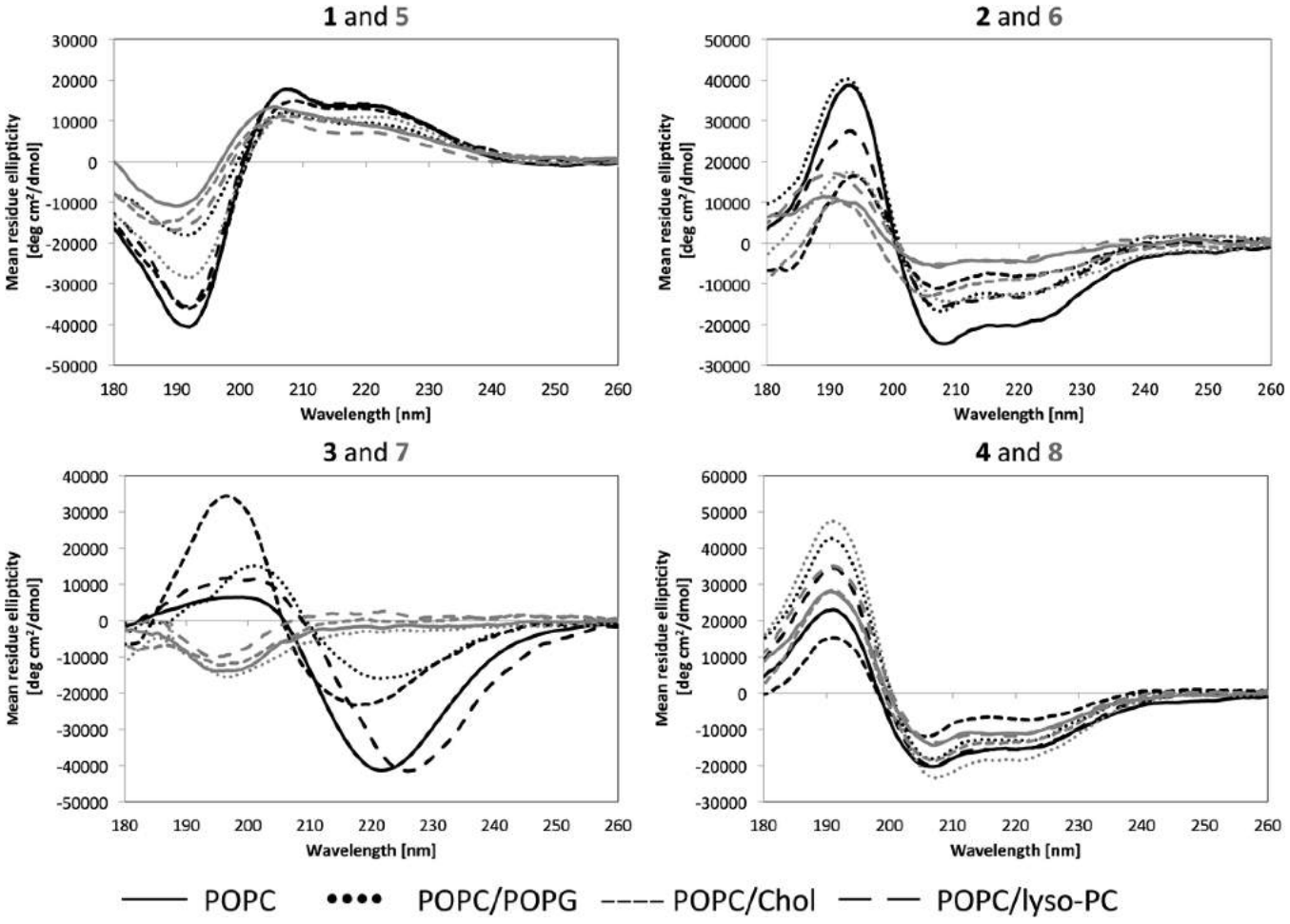

Figure 4. Synchrotron radiation CD spectra of the linear CPPs **1**, **2**, **3**, and **4** and their stapled analogues **5**, **6**, **7**, and **8** in the presence of small unilamellar lipid vesicles with different compositions (all molar peptide-to-lipid ratios were 1:50, temperature of 30 °C). Spectra of the stapled analogues are represented by gray lines.

conformational restriction was imposed around a helix-breaking proline residue. It is conceivable that this flexible linker might have otherwise facilitated a more ideal adaptation of the amphiphilic peptide structure to the membrane environment.

In the case of **2** (Figure 4) the α-helix content decreased from an average of 50% [POPC 57%; POPC/POPG 67%; POPC/lysoPC 42%; POPC/Chol 34%] to around 22% in **6** [POPC 13%; POPC/POPG 32%; POPC/lysoPC 15%; POPC/Chol 27%]. Also in this case, it seems that the decrease may be attributed to an interference of the lactam staple with the optimal membrane-adapted helical fold, given that the CD signal intensities of **6** in lipids are the same or even less than the ones in water. Hence, the highest helicity is manifest in the linear **2** peptide when bound to membranes.

For **3** and **7** (Figure 4) the quality of the fit between experimental and back-calculated spectrum led to normalized root-mean-square deviations higher than 0.1 and therefore did not allow for accurate calculation of secondary structure content. However, the spectral line shapes of **3** in POPC/Chol suggest mixed α-helix and β-sheet content. In POPC, POPC/POPG and POPC/lysoPC **3** seems to adopt β-pleated conformations. The strong absorption flattening at short wavelengths indicates that **3** is possibly β-aggregated. Interestingly, the results of the stapled analogue **7** suggest that the staple, which had been designed to stabilize an α-helix, actually prevents the folding into an α-helical conformation. The typical random coil line shape of **7** suggested that the conformationally restricted peptide does not bind at all to lipid membranes; hence the situation is essentially the same as that in pure aqueous solutions. The linear **3**, on the other hand, can bind very well to the various kinds of lipid membranes by adopting a partial β-pleated conformation.

For the linear **4** (Figure 4), an α-helix is obviously the preferred conformation in a membrane environment, as expected from its secondary amphiphilic character, being most pronounced in the lipid composition POPC/POPG. While the average α-helix content increased 3% from 43% for the linear peptide **4** [POPC 38%; POPC/POPG 58%; POPC/lysoPC 47%; POPC/Chol 27%], it did not change significantly for the restrained analogue **8** with an average of 46% [POPC 37%; POPC/POPG 59%; POPC/lysoPC 45%; POPC/Chol 43%].

Membrane Disruption. As our main intention was to examine the stapled peptides as CPPs, we next examined their ability to perturb lipid bilayers. Using large unilamellar vesicles, we determined the peptide-induced leakage of an entrapped fluorescent dye to find out whether stapling would affect membrane integrity. The fluorescence dequenching experiments were performed with vesicles of two different lipid compositions: uncharged POPC and a mixture of POPC/

DOI: 10.1021/acs.jmedchem.7b00813
J. Med. Chem. 2017, 60, 8071−8082

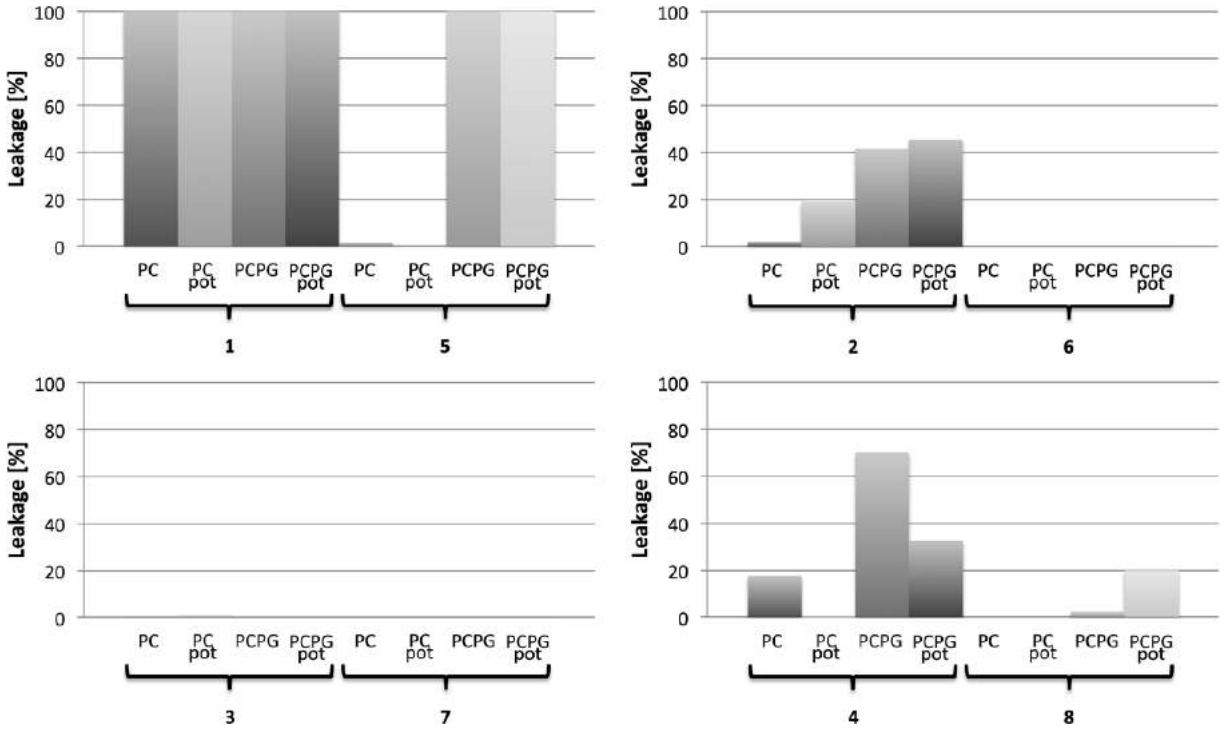

Figure 5. Disruption of lipid vesicles consisting of POPC (PC) and POPC/POPG (PCPG) induced by the linear CPPs **1**, **2**, **3**, and **4** and their stapled analogues **5**, **6**, **7**, and **8**. Vesicles were incubated with the peptides at a peptide-to-lipid ratio of 1:25 at a temperature of 30 °C, without and with an applied membrane potential of −120 mV (pot) for 30 min. Disruption is expressed in percent of 100% leakage induced by TritonX-100.

Table 2. Minimum Inhibitory Concentrations of the Linear CPPs 1, 2, 3, and 4 and Their Stapled Analogues 5, 6, 7, and 8[a]

	MIC (μg/mL) for peptides							
strain	**1**	**5**	**2**	**6**	**3**	**7**	**4**	**8**
E. coli	32	32	256	>256	>256	>256	16	64
P. aeruginosa	64	64	>256	>256	>256	>256	256	>256
S. aureus	32	128	16	>256	>256	>256	16	256
E. faecalis	32	64	64	>256	>256	>256	256	>256

[a]Data are expressed as mean of two independent experiments.

POPG (3/1, mol/mol) (Figure 5). As shown above, the presence of an anionic phospholipid caused the highest helicity in those stapled peptides that would assume a (partially) helical conformation in membranes per se because electrostatic attraction helps to accumulate the cationic peptides on the membrane surface. To study the influence of electrostatics also on the subsequent step of membrane permeabilization, all fluorescence experiments were carried out with and without applying a transmembrane potential of 120 mV (negative inside). The translocation of cationic peptides should be additionally increased by this potential, which was generated by valinomycin (an ionophor) and a replacement of K^+ in the outside buffer by Na^+. The lipid and peptide concentrations were 50 μM and 2 μM, respectively.

As a general trend, the linear CPPs caused more leakage from the vesicles than their stapled analogues. **1** and **5** (Figure 5) gave 100% leakage except for **5** in pure POPC and in POPC with a membrane potential (Figure 5) where stapling actually prohibited leakage. Membrane permeabilization by **1** is not surprising, as this melittin derivative is a known cytolytic peptide.[26] Membrane potential had no effect on **1** in POPC/POPG or on **3**/**7** in any membrane system. By comparison, the potential was found to enhance leakage for **2**, and it lowered the membranolytic action of **4**. For POPC membranes, **6** and **8** were less lytic than their linear counterparts, also in the presence of membrane potential. Only for POPC/POPG vesicles, the additional membrane potential led to a further elevation of leakage by stapled **8** (Figure 5).

Antimicrobial Activity. Next, we examined the membrane perturbing effect of the linear CPPs and their stapled analogues on living bacteria by determining the minimum inhibitory concentration (MIC). To characterize the bacteriostatic activity of the peptides, we used a standard broth dilution assay with two Gram-negative strains (*Escherichia coli*, *Pseudomonas aeruginosa*) and with two Gram-positive strains (*Staphylococcus aureus*, *Enterococcus faecalis*).[42]

Generally, stapling did not enhance the antimicrobial activity for any of the peptides. The peptides **1** and **5** had the same growth inhibiting effect on Gram-negative bacteria and in Gram-positive ones. **5** was slightly less active compared to its linear form (Table 2). The linear peptide **2** was active toward Gram-positive strains, while in the stapled form **6** showed no inhibition on either Gram-negative or Gram-positive bacteria. Also for **4**, stapling (**8**) resulted in a drop of antimicrobial activity against all bacteria. Neither linear **3** nor **7** had any effect on bacterial growth. Even though we did not explicitly confirm that the inhibitory activity was due to membrane leakage, these

DOI: 10.1021/acs.jmedchem.7b00813
J. Med. Chem. 2017, 60, 8071−8082

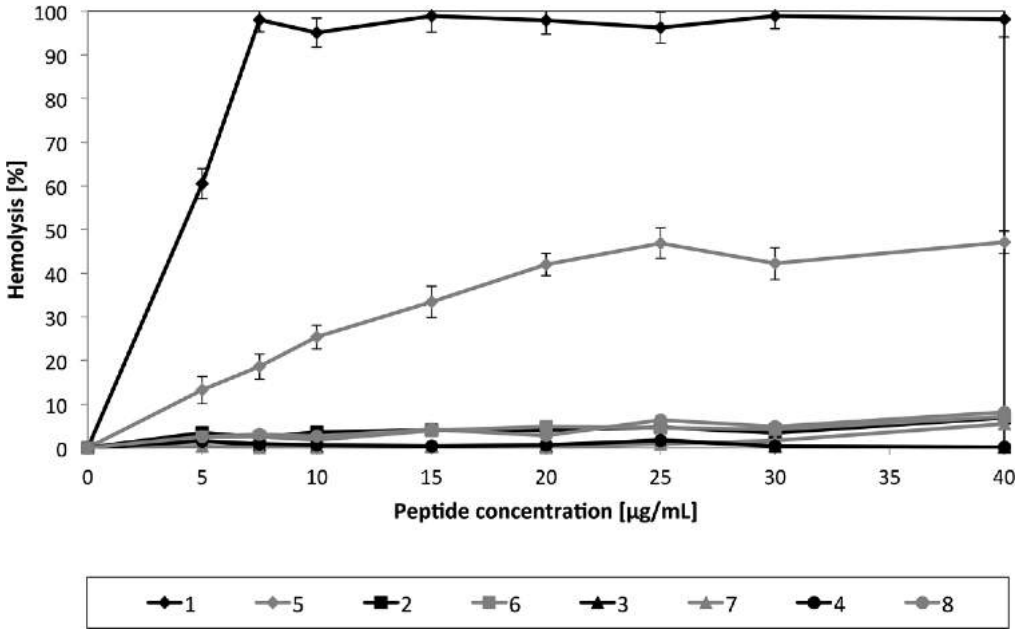

Figure 6. Hemolysis of human red blood cells upon treatment with the linear CPPs **1**, **2**, **3**, and **4** and their stapled analogues **5**, **6**, 7, and **8** as a function of peptide concentration. Data are expressed as the mean ± SD of two independent experiments.

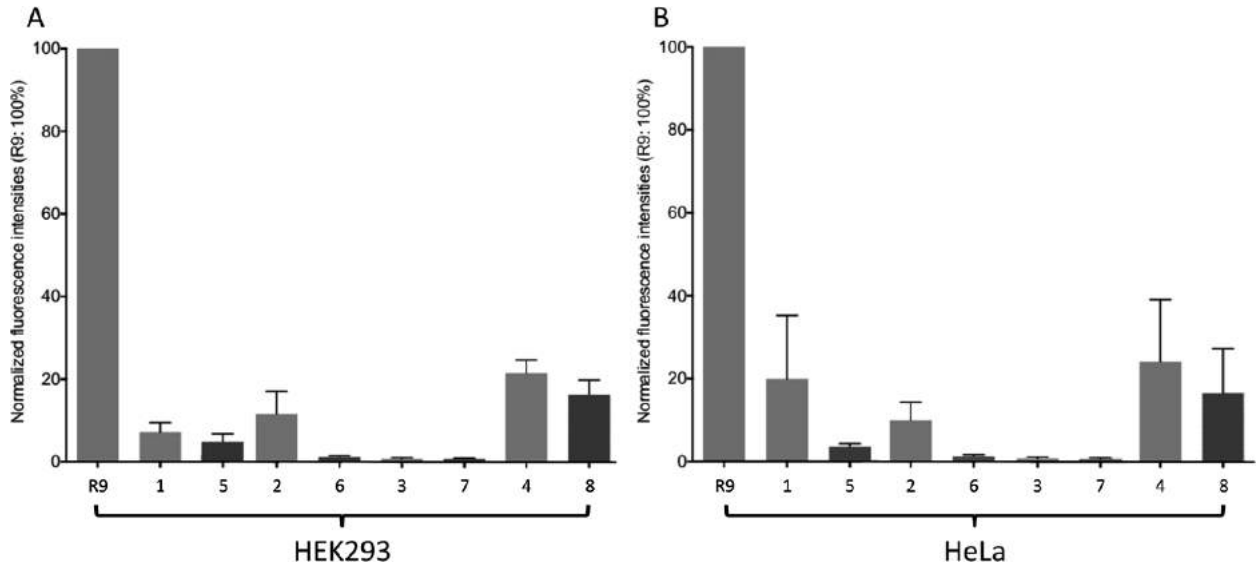

Figure 7. Cell uptake, as monitored by flow cytometry, of the four fluorescent-labeled CPPs and their stapled counterparts in HEK293 cells (A) and HeLa cells (B). The fluorescence intensities are normalized relative to the signal of carboxyfluorescein-labeled R9. Cells were incubated with the peptides at a concentration of 2 μM for 4 h in serum-free medium. Before the measurement, trypan blue (0.4% end concentration) was administered to quench cell surface-bound fluorescence and restrict the recorded signal to intracellular fluorescence. Each bar represents the mean value of two independent experiments ± SD.

results are in line with the reduced membrane-disruptive capacity in the vesicle assay.

Hemolysis. As a further well-established test for membrane-disruptive activity, we performed hemolysis experiments. All peptides caused a certain permeabilization of these eukaryotic membranes. However, again the maximum value of hemolysis reached by each stapled peptide was similar to or less than the value of its linear analogue. The results for **1** illustrate the typical problem faced when exploring membranolytic peptides for therapeutic applications, as the high hemolytic activity of melittin excludes its use in systemic applications.[26] Both **1** and **5** caused hemolysis at a concentration of 10−40 μg/mL, but the stapled analogue reached only about 50% lysis compared to 100% by the linear form (Figure 6).

Uptake into Tissue Culture Cells. Ultimately, we were interested to learn whether lactam stapling promoted uptake into mammalian cells. Flow cytometry for fluorescein labeled analogues was performed with two adherent cell lines, HEK and HeLa cells, to monitor the peptide uptake in tissue culture. For referencing, we included nonaarginine (R9) as a well-characterized and highly active CPP. All peptides were less active than R9, and in each case the activity of the linear peptide exceeded the one of the stapled counterpart (Figure 7). However, when comparing these relative changes in cell-

DOI: 10.1021/acs.jmedchem.7b00813
J. Med. Chem. 2017, 60, 8071−8082

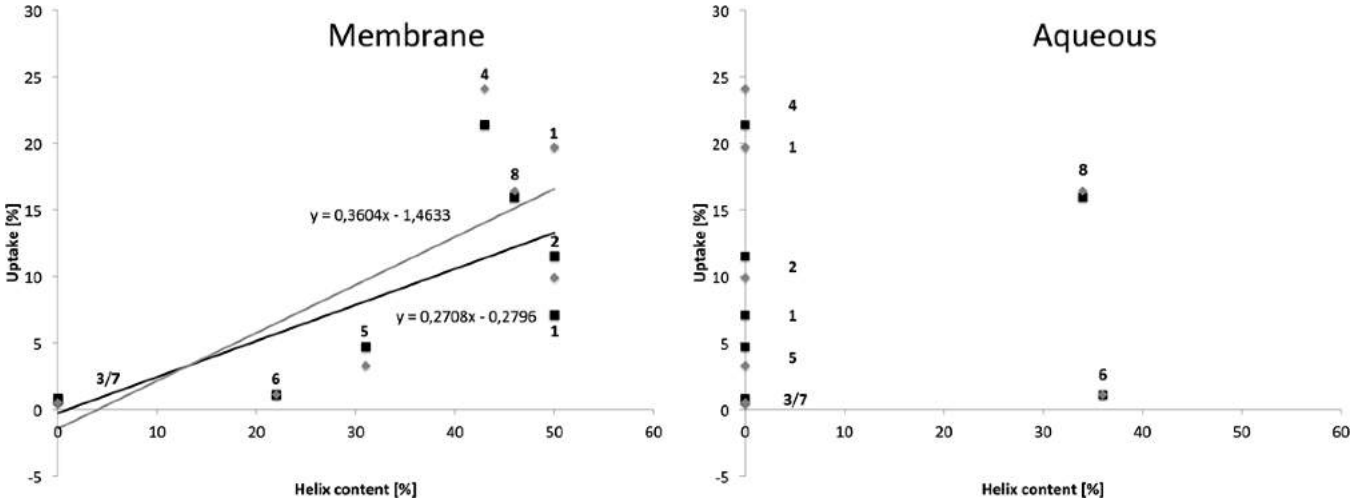

Figure 8. Correlation between the observed α-helix content in the four CPPs **1**, **2**, **3**, and **4** and their stapled analogues **5**, **6**, **7**, and **8** when bound to membranes or in aqueous solution, and their corresponding cell uptake in HEK293 cells (■) and HeLa cells (◆). Linear trend lines illustrate the correlation.

penetrating activity in living cells with the disruptive effects on model membranes above, a greater reduction in activity occurred in the model systems, especially for **4** and its constrained analogue **8**. In the cases of **1** and **5** we also observed a similar situation when correlating the uptake into HEK293 cells and the reduced disruption of POPC vesicles.

■ DISCUSSION

So far, peptide stapling has been primarily concerned with enhancing the activity of peptidic inhibitors of protein−protein interactions that involve helical interaction domains.[43] In particular, peptides that are conformationally constrained by a hydrocarbon staple also possess an intrinsic capacity to enter cells and reach their target in the cytosol.[44] It has been acknowledged that stapling does not present a generic solution for enhanced uptake and activity, as the position of the staple is critical.[45] For arginine-rich CPPs, conformational restriction through end-to-end cyclization was shown to promote direct membrane permeation.[46]

To this point, there have been no studies about the relationship between stapling of a cell-penetrating peptide by a lactam bridge and relevant functional aspects. We thus used a broad experimental approach to address issues that are relevant in the process of cell penetration, ranging from structural analysis in solution, over lipid interactions in model bilayers, to membrane damage and uptake in living cells. We introduced a lactam bridge into suitable positions of the peptides such that folding into an α-helical conformation should be encouraged already before the actual contact with lipid membranes. In this way, we reasoned that the uptake in cells might possibly be facilitated compared to the linear analogues. Given that for amphipathic peptides helicity had been correlated with enhanced capacity to perturb/insert into membranes,[22,47] it was surprising to find that membrane binding was drastically decreased for all peptides upon introducing a lactam bridge. These consequences clearly emerged from our biophysical leakage assay and from the data we gained in experiments with bacteria and red blood cells. For neither one of the four representative CPPs, stapling enhanced the properties related to CPP-bilayer interactions. For **1** and **3** this observation may be explained by the fact that stapling did not lead to a helix preformation in aqueous solution. Overall, **3** is not so suitable as a CPP due to its hydrophobicity and its tendency to form β-aggregates. Even though the aggregation was hampered by the staple in dilute samples (Figure 3), at higher concentrations (used in most of the bioassays) this inhibition of aggregation was insufficient to improve cell uptake. However, the failure of stapling to enhance uptake also holds for the two cases of **2** and **4**, where stapling had converted the unstructured peptides in solution into their functionally relevant amphipathic α-helical conformations according to expectations. Taking into consideration that reducing the helix forming propensity strongly impairs uptake,[22] we expected an increased internalization of these peptides. However, the helix content of **6** dropped in membranous environments compared to its linear form. Furthermore, even in the case of **8**, where lactam-stapling increased the helix content in aqueous as well as membranous systems, uptake could not be improved.

Overall, these results show that secondary structure stabilization per se does not provide a rational approach to enhance activity as a CPP. Other factors need to be considered as well if we compare the placement of our lactam bridge on the hydrophobic/hydrophilic border of an amphiphilic α-helix with previous work, where hydrocarbon staples were positioned on the hydrophobic face.[19] A hydrocarbon staple increases the hydrophobic surface of a peptide and thereby its overall hydrophobicity, which will enable the peptide to insert more deeply into the lipid bilayer core, compared to the polar amide bond of a lactam bridge. Given that a lactam bridge does not increase the hydrophobic surface, it should not affect membrane binding to such an extent and rather reveal any structural effects more directly.[19] Therefore, we consider this staple a better suited approach to single out the impact of helix stabilization on uptake.

By use of flow cytometry, the toxicity toward HEK293 and HeLa cells could also be determined. We can clearly conclude that at the used concentrations none of our peptides, neither the linear nor the stapled forms, showed any cytotoxicity.

Excitingly, the impact of the staple varied for individual activities, which for **4**/**8** led to an improvement of the overall characteristics. Lysis in the leakage experiments, especially for

DOI: 10.1021/acs.jmedchem.7b00813
J. Med. Chem. 2017, 60, 8071−8082

POPC/POPG vesicles, was reduced by almost 100% while cell uptake was reduced by only 30%.

Next, we analyzed our data to find any meaningful correlation between the various structural properties and the ensuing functional consequences. Interestingly, the α-helix content of the peptides when bound to lipid membranes was found to correlate remarkably well with their uptake in HEK293 and HeLa cells (Figure 8). The coefficient of determination (R2) of the linear regression indicates for both cell lines a relatively good fit (R2(HEK) = 0.938, R2(HeLa) = 0.924). In contrast, there was no correlation between the degree of helicity measured in aqueous solution and their internalization into cell (Figure 8). The latter finding is not surprising, given that six out of our eight peptides did not adopt any secondary structure in aqueous solution at all (Figure 3). Even for the two successfully stapled analogues (**6** and **8**), their uptake differed considerable despite the very similar helicity reached (Figure 8). Overall, these results clearly demonstrate that the intrinsic helicity of a CPP in solution has little impact on its cell penetrating activity, whether stapled or not, but it is rather the helical fold upon membrane contact that serves as a relevant predictor of activity.[22,47]

Overall, our data suggest that the conformational freedom of folding into a suitable secondary structure seems to be more critical for cell uptake than saving the entropic costs of binding by preforming a stapled helix. A recent study of the arginine-rich CPP pituitary adenylate-cyclase-activating polypeptide has indicated that an induced random-coil-to-α-helix conversion plays an important role in the process of glycosaminoglycan-mediated internalization.[48] We can thus extend this concept now and suggest that the conformational conversion upon membrane binding is relevant not only for that particular class of arginine-rich CPPs but also for the internalization of α-helical amphipathic CPPs. Next, it will be interesting to move the location of the staples in our peptides to include hydrocarbon/thioether/triazole staples and to study other types of stapled CPPs in order to see whether any these measures lead to an enhanced or reduced cell uptake and whether our conclusions from the current set of data can be generalized more widely.

EXPERIMENTAL SECTION

Peptide Synthesis. Peptide synthesis reagents and Fmoc-protected amino acids were purchased from Merck Biosciences (Darmstadt, Germany) and/or Iris Biotech (Marktretwitz, Germany). Solvents for peptide synthesis were purchased from Merck (Darmstadt, Germany) or from Biosolve (Valkenswaard, The Netherlands), and solvents for HPLC purification were obtained from Fischer Scientific (Geel, Belgium). The peptides were synthesized by manual solid peptide synthesis employing 9-fluorenylmethyloxy (Fmoc) chemistry. Fmoc-protected amino acids were coupled as 1-hydroxybenzotriazole esters in the presence of benzotriazol-1-yloxytripyrrolidinophosphonium hexafluorophosphate and *N*,*N*-diisopropylethylamine on 4-((2,4-dimethoxyphenyl)(Fmoc-amino)methyl)phenoxyalkyl resin to generate C-terminally amidated peptides. Peptides were deprotected with 20% piperidine in *N*,*N*-dimethylformamide for 30 min. Mass spectra were recorded on an Autoflex III instrument (Bruker-Daltonik, Germany). Reverse-phase high-performance liquid chromatography (HPLC) was performed on an HPLC system with PU-2080 Plus pumps and a diode-array UV detector (Jasco, Groß-Umstadt, Germany). Vydac polymeric C18 columns from Grace Davidson Discovery Science (Columbia, MD, USA) were employed (4.6 mm × 250 mm as analytical, 10 mm × 250 mm as semipreparative). Linear gradients, using as solvent A: 90% water and 10% acetonitrile. Solvent B: 90% acetonitrile, 10% water. 0.1% trifluoroacetic acid was used as an ion-pairing agent in all cases. The stapled analogues and the N-terminally 5(6)-carboxyfluorescein-labeled analogues of the peptides were synthesized by CS Bio Co. (Menlo Park, CA, USA).

The purity of peptides was confirmed by LC−MS using an 1100 series LC system (Agilent, Waldbron, Germany) coupled to an ESI mass spectrometer μTOF mass spectrometer (Bruker Daltonics, Bremen, Germany), on a C18 analytical column (Grace Vydac, 300 Å, 5 μm, 250 mm × 2.1 mm), using a linear gradient of 5% acetonitrile in 0.1% trifluoroacetic acid to 95% acetonitrile in 0.1% trifluoroacetic acid over 24 min at a flow rate of 0.30 mL/min. All peptides were found to be over 95% pure.

Preparation of Lipid Vesicles. The lipids 1-palmitoyl-2-oleoyl-*sn*-glycero-3-phosphocholine (POPC), 1-palmitoyl-2-oleoyl-*sn*-glycero-3-phospho-(1′-*rac*-glycerol) (POPG), 1-palmitoyl-2-hydroxy-*sn*-glycero-3-phosphocholine (lysoPC), and 1,2-dioleoyl-*sn*-glycero-3-phosphoethanolamine-*N*-(lissamine rhodamine B sulfonyl) (Rhod-PE) were purchased from Avanti Polar Lipids (Alabaster, AL, USA). 8-Aminonaphthalene-1,3,6-trisulfonic acid (ANTS) and *p*-xylene-bis-pyridinium bromide (DPX) were from Invitrogen, Karlsruhe, Germany. Cholesterol (Chol) was purchased from Sigma-Aldrich (Munich, Germany), and phosphate buffer (PB) was obtained from VWR (Darmstadt, Germany). Large unilamellar vesicles (LUVs) and small unilamellar vesicles (SUVs) were utilized for fluorescence spectroscopy and CD analysis, respectively. In order to observe any effect from lipids with negatively charged head groups, lipid curvature, or membrane structural integrity and fluidity, we employed different mixtures of bilayer components. Weighted amounts of lipids were dissolved in $CHCl_3$/methanol (1/1, v/v), and the solvents were dried under a gentle nitrogen stream. Finally, residual solvent was removed under vacuum overnight.

The dried lipid was then hydrated by a buffer containing the fluorescent dye ANTS and the quencher DPX for the leakage experiments or phosphate buffer for the CD measurements. After 10 freeze−thaw cycles and vigorous vortexing between each cycle, multilamellar vesicles (MLVs) were obtained. For CD analysis MLVs were converted to SUVs by sonication in a high-power ultrasonic bath (UTR 200, Hielscher Ultrasonic, Teltow, Germany) while keeping the bath temperature constant at 30 °C. To obtain LUVs for the leakage experiments the corresponding MLVs were extruded 21 times through a polycarbonate membrane with pore size of 100 nm (Avanti, Mini-Extruder).

Circular Dicroism (CD) Spectroscopy. Conventional CD spectroscopy was also employed for samples in aqueous solution (deionized water, phosphate buffer (10 mM, pH 7.4) or phosphate buffer + NaF (100 mM)). Spectra were recorded on a J-815 spectropolarimeter (Jasco, Groß-Umstadt, Germany). Weighed amounts of peptide were directly dissolved in the different aqueous solutions to obtain the CD samples. Measurements were performed on a 260 μL aliquot with ∼0.03 μmol/mL in quartz glass cells (Suprasil, Hellma, Müllheim, Germany) of 1 mm path length between 260 and 180 at 0.1 nm intervals. Spectra were recorded at 30 °C using a water-thermostated rectangular cell holder. Three repeat scans at a scan rate of 10 nm/min, 8 s response time, and 1 nm bandwidth were averaged for each sample and for the baseline of the corresponding peptide-free sample. After subtraction of the baseline from the sample spectra, CD data were processed with the adaptive smoothing method, which is part of the Jasco Spectra Analysis software.

Synchrotron radiation CD (SRCD) was used to investigate the secondary structure of the peptides reconstituted in lipid vesicles, because of the strong background absorption of the unsaturated lipids and the unfavorable scattering of the SUVs that lead in general to poor spectral quality. SRCD spectra were collected at the UV-CD12 beamline of the ANKA storage ring (KIT, Germany). The beamline components and its experimental end-station have been described in detail recently.[49]

CD samples were prepared by cosolubilizing POPC, POPC/POPG(3/1), POPC/Chol(3/1), or POPC/lysoPC (9/1) with the peptides in $CHCl_3$/methanol (1/1, v/v). A peptide-to-lipid molar ratio of 1/50 was used for the measurements, resulting in peptide

DOI: 10.1021/acs.jmedchem.7b00813
J. Med. Chem. 2017, 60, 8071−8082

concentrations of 1 μmol/mL and lipid concentrations of 50 μmol/mL, respectively. SUVs were prepared as described above. Measurements were performed on a 3.5 μL aliquot of the sample in a "Birkbeck-type" demountable CaF_2 cell with a path length of 7.2 μm (Hellma, Müllheim, Germany), acquiring the spectrum between 260 and 180 at 0.5 nm intervals.[50] Spectra were recorded at 30 °C, using a cell holder thermostated by Peltier elements. A scan rate of 15 nm/min, 1 nm spectral bandwidth, 0.3 s lock-in time constant, and 1.5 s dwell time were applied. Three spectra were acquired and averaged for each sample. The average spectrum was corrected by subtracting the corresponding spectrum of SUV dispersion in the absence of peptide.

For better comparison of the spectra of the different samples, the calculated mean residue ellipticity (MRE) is shown in the graphs for the lipid vesicle samples. Secondary structure analyses were performed using the CDSSTR program with the implemented singular value decomposition algorithm and by the CONTIN-LL program, which is based on the ridge regression algorithm.[36−38] The two algorithms are provided by the DICHROWEB online server.[39−41] The quality of the fit between experimental and back-calculated spectrum according to the secondary structure fractions was assessed from the normalized root-mean-square deviation, with a value of <0.1 considered as a good fit.[40]

Vesicle Leakage Assay. The leakage experiments were performed according to an assay introduced by Ellens et al. (1984) by which the efflux of an encapsulated dye can be followed due to its dequenching.[51] The buffer in which the vesicles had been prepared contained the fluorophore (12.5 mM 8-aminonaphthalene-1,3,6-trisulfonic acid (ANTS)), the quencher (45 mM *p*-xylene-bis-pyridinium bromide (DPX)), 52 mM K_2SO_4, and 10 mM piperazine-*N*,*N*′-bis(2-ethanesulfonic acid) (PIPES) (pH 7.0). ANTS and DPX were from Invitrogen (Karlsruhe, Germany). TritonX-100 and PIPES were from Sigma-Aldrich (Munich, Germany). The fluorophore and quencher that were not entrapped within the vesicles were removed by size exclusion chromatography using spin columns (Pierce centrifuge column, 2 mL, Life Technologies GmbH, Darmstadt, Germany) filled with Sephacryl 100-HR (Sigma-Aldrich, Munich, Germany) (2 min, 1500*g*). A 10 mM PIPES buffer (pH 7.0) containing 110 mM K_2SO_4 to balance the osmolarity was used for elution and for the measurements. After extrusion and the removal of the external dye and quencher, the lipid concentration usually decreases. Therefore, to quantify the lipid loss, 0.02 mol % Rhod-PE had been added to the lipid stock solutions, and before each set of measurements, a rhodamine spectrum was recorded to determine the actual concentration of lipids, which was referenced to a spectrum of vesicles prepared by sonication without any subsequent treatment.

The fluorescence measurements were performed on a FluoroMax2 spectrofluorimeter (HORIBA Jobin Yvon, Unterhaching, Germany) equipped with a thermostated sample holder and magnetic stirrer using an excitation wavelength of 355 nm, an emission wavelength of 515 nm, and spectral band widths of 5 nm each. The peptide solutions were placed in elution buffer in a 1 cm standard cuvette. One hundred seconds after the start of the measurement, the lipid vesicles were added, and the intensity of the fluorescence at 515 nm was recorded. The leakage was measured for 600 s after the addition of the vesicles, and the measurement was terminated after addition of Triton-X-100 solution in Milli-Q water (0.25% v/v), which dissolved the vesicles and yielded 100% leakage. To determine the background signal of the vesicles themselves, several blanks were recorded in each set of measurements. When an additional membrane potential (120 mV/negative inside) has been applied, potassium in the outside buffer was replaced by sodium, and the vesicles were added first together with 25 nM valinomycin (Sigma-Aldrich, Munich, Germany).

Minimum Inhibitory Concentration (MIC) Determination. Antimicrobial activity was tested as a minimum inhibitory concentration, according to the standard broth microdilution assay performed with some modifications.[52] Bacterial strains *Escherichia coli* DSM 1103 (ATCC 25922), *Pseudomonas aeruginosa* DSM 1117 (ATCC 27853), *Staphylococcus aureus* DSM 1104 (ATCC 25923), and *Enterococcus faecalis* DSM 2570 (ATCC 29212) were obtained from the German Collection of Microorganisms and Cell Cultures (DSMZ, Braunschweig, Germany). The bacterial strains were maintained frozen at −80 °C using bacterial Cryobank System (Mast Diagnostica, Reinfeld, Germany). To refresh bacterial cells on single glass beads, they were grown overnight in Mueller−Hinton (MH) broth. In a further step, the colonies were obtained by streaking on MH agar. Then colony cells were used for inoculation of MH broth up to OD = 0.02 and grown at 37 °C overnight. The overnight cultures were used to inoculate the test culture, which was grown 3−4 h in order to reach exponential growth.

We prepared the peptide stock solution in 50% EtOH. This solvent system, according to our experience, has never influenced bacterial growth (multiple control experiments). The 96-well microtiter plates Nunclon (Nunc GmbH & Co., Wiesbaden, Germany) were filled with 50 μL of MH broth, and consecutive 2-fold dilutions of peptides were arranged in triplicates. Two independent experiments were performed with equal results. The two final rows of each plate remained without peptide so that the penultimate data point served as the positive control (no peptide) and the final one as the negative control (not inoculated). The plates were incubated at 37 °C for 22 h, and the MIC was determined visually after addition of 20 μL of resazurin (80 μM) and additional cultivation for 2 h. The pink-colored reduced form (resorufin) indicates active respiration and bacterial growth. The remained-blue-colored oxidative form of resazurin points to the growth inhibition. Two independent experiments were performed with equal results.

Hemolysis Assay. Hemolytic activity was examined with a consecutive 2-fold dilution assay. Citrate phosphate dextrose-stabilized blood bags with erythrocyte suspensions were obtained from the blood bank of the local municipal hospital (Karlsruhe, Germany). The previously washed erythrocytes were gently shaken during incubation with peptide solution at 37 °C for 30 min. The mixture was centrifuged at 13 000 rpm for 10 min to precipitate the cells, and the absorbance of the supernatant was recorded at 540 nm against a negative control, performed only in reaction buffer to exclude the influence of autohemolysis and/or mere cells. The percentage of the lysis of the erythrocytes was determined in relation to the 100% value of hemolysis in buffer (with 0.1% Triton X-100). The absorbance measurements were performed in triplicates and in two independent experiments, and the average values were used for calculation.

Cell Cultures. HEK293 (ATCC CRL-3216) and HeLa (ATCC CCL-2) cells were maintained in Gibco DMEM and Gibco RPMI 1640 medium (Thermo Fisher Scientific, Waltham, MD, USA), respectively, supplemented with 10% fetal calf serum (FCS, PAN Biotech, Aidenbach, Germany). All cells were incubated at 37 °C in a 5% CO_2-containing, humidified incubator. Cells were passaged every 2−3 days. All cells were originally obtained from the American Type Culture Collection (Rockville, MD, USA).

Fluorescence-Activated Cell Sorting (FACS) Analysis. The cells were seeded in 48-well plates (Sarstedt, Numbrecht, Gemany) at a density of 40 000 cells/well 1 day prior to the experiment. The next day a premix of cell culture medium without phenol red and FCS, containing 2 μM of the indicated peptides, was prepared and transferred to the 48-well plates followed by an incubation for 4 h at 37 °C. Afterward the cells were detached with 2 mM ethylenediaminetetraacetic acid in 1× phosphate buffered saline (pH 7.4), washed gently 3 times with prewarmed DMEM without phenol red and FCS. Propidium iodide was included as marker for late apoptosis at a concentration of 2.5 μg/mL. HEK293 and HeLa cells were transferred to flow cytometry tubes (Micronic B.V., Lelystad, The Netherlands) immediately after finishing the confocal imaging, and flow cytometry was performed. Flow cytometry data of cells were aquired using a BD FACS-Calibur (BD Biosciences, Erembodegem, Belgium) flow cytometer with a 488 nm argon ion laser using spectral ranges 530/40 for fluorescein and 613/20 for propidium iodide. FCS Express version 4 Research Edition (De Novo Software, Los Angeles, CA, USA) was used for the analysis of the generated data. Per sample, <4000 morphologically intact cells were gated based on forward versus sideward scatter and analyzed. Before measuring, trypan blue (0.4% end concentration) was administered to quench cell surface-bound fluorescence and restrict the recorded signal to intracellular

DOI: 10.1021/acs.jmedchem.7b00813
J. Med. Chem. 2017, 60, 8071−8082

fluorescence. Two independent experiments were performed, and average values were used for calculation.

■ ASSOCIATED CONTENT

Supporting Information

The Supporting Information is available free of charge on the ACS Publications website at DOI: 10.1021/acs.jmedchem.7b00813.

Figure S1 showing leakage data of the linear CPPs **1**, **2**, **3**, and **4** and their stapled analogues **5**, **6**, **7**, and **8** at different peptide-to-lipid ratios (PDF)

■ AUTHOR INFORMATION

Corresponding Author

*E-mail: anne.ulrich@kit.edu. Phone: +49 721 608 43222. Fax: +49 608 44823.

ORCID

Parvesh Wadhwani: 0000-0002-7290-5154

Roland Brock: 0000-0003-1395-6127

Anne S. Ulrich: 0000-0001-5571-9483

Notes

The authors declare no competing financial interest.

■ ACKNOWLEDGMENTS

M.J.K. and S.S. were supported by postdoctoral fellowships (RPF) from Roche Pharma Research and Early Development, Pharmaceutical Sciences, Roche Innovation Center Basel, F. Hoffmann-La Roche Ltd, Grenzacherstrasse 124, 4070 Basel, Switzerland. We thank the Synchrotron Light Source ANKA for providing beam time at the UV-CD12 beamline, and Siegmar Roth and Bianca Posselt for technical assistance in using the beamline and the sample preparation lab.

■ ABBREVIATIONS USED

CPP, cell-penetrating peptide; MAP, model amphipathic peptide; NMR, nuclear magnetic resonance; TAT, transactivator of transcription; CHO, Chinese hamster ovary; SAP, sweet arrow peptide; PB, phosphate buffer; POPC, 1-palmitoyl-2-oleoyl-*sn*-glycero-3-phosphocholine; POPG, 1-palmitoyl-2-oleoyl-*sn*-glycero-3-phospho-(1′-*rac*-glycerol); Chol, cholesterol; lysoPC, 1-palmitoyl-2-hydroxy-*sn*-glycero-3-phosphocholine; SRCD, synchrotron radiation circular dichroism; MIC, minimum inhibitory concentration; HEK, human embryonic kidney; HeLa, Henrietta Lacks; HPLC, high-performance liquid chromatography; Rhod-PE, 1,2-dioleoyl-*sn*-glycero-3-phosphoethanolamine-*N*-(lissamine rhodamine B sulfonyl); DPX, *p*-xylene-bis-pyridinium bromide; ANTX, 8-aminonaphthalene-1,3,6-trisulfonic acid; MLV, multilamellar vesicle; PIPES, piperazine-*N*,*N*′-bis(2-ethanesulfonic acid); MH, Mueller–Hinton; DMEM, Dulbecco's modified Eagle's medium; RPMI, Roswell Park Memorial Institute; FCS, fetal calf serum

■ REFERENCES

(1) Milletti, F. Cell-penetrating peptides: classes, origin, and current landscape. *Drug Discovery Today* **2012**, *17*, 850–860.

(2) Pooga, M.; Langel, Ü. Classes of Cell-Penetrating Peptides. In *Cell-Penetrating Peptides: Methods and Protocols*; Langel, Ü., Ed.; Springer: New York, 2011; pp 3–28.

(3) Lönn, P.; Dowdy, S. F. Cationic PTD/CPP-mediated macromolecular delivery: charging into the cell. *Expert Opin. Drug Delivery* **2015**, *12*, 1627–1636.

(4) Morris, M. C.; Vidal, P.; Chaloin, L.; Heitz, F.; Divita, G. A new peptide vector for efficient delivery of oligonucleotides into mammalian cells. *Nucleic Acids Res.* **1997**, *25*, 2730–2736.

(5) Morris, M. C.; Depollier, J.; Mery, J.; Heitz, F.; Divita, G. A peptide carrier for the delivery of biologically active proteins into mammalian cells. *Nat. Biotechnol.* **2001**, *19*, 1173–1176.

(6) El-Andaloussi, S.; Holm, T.; Langel, U. Cell-penetrating peptides: mechanisms and applications. *Curr. Pharm. Des.* **2005**, *11*, 3597–3611.

(7) Nakase, I.; Hirose, H.; Tanaka, G.; Tadokoro, A.; Kobayashi, S.; Takeuchi, T.; Futaki, S. Cell-surface accumulation of flock house virus-derived peptide leads to efficient internalization via macropinocytosis. *Mol. Ther.* **2009**, *17*, 1868–1876.

(8) Derossi, D.; Calvet, S.; Trembleau, A.; Brunissen, A.; Chassaing, G.; Prochiantz, A. Cell internalization of the third helix of the Antennapedia homeodomain is receptor-independent. *J. Biol. Chem.* **1996**, *271*, 18188–18193.

(9) Matsuzaki, K.; Yoneyama, S.; Murase, O.; Miyajima, K. Transbilayer transport of ions and lipids coupled with mastoparan X translocation. *Biochemistry* **1996**, *35*, 8450–8456.

(10) Pouny, Y.; Rapaport, D.; Mor, A.; Nicolas, P.; Shai, Y. Interaction of antimicrobial dermaseptin and its fluorescently labeled analogues with phospholipid membranes. *Biochemistry* **1992**, *31*, 12416–12423.

(11) Lee, M. T.; Hung, W. C.; Chen, F. Y.; Huang, H. W. Many-body effect of antimicrobial peptides: on the correlation between lipid's spontaneous curvature and pore formation. *Biophys. J.* **2005**, *89*, 4006–4016.

(12) Thoren, P. E.; Persson, D.; Isakson, P.; Goksor, M.; Onfelt, A.; Norden, B. Uptake of analogs of penetratin, Tat(48-60) and oligoarginine in live cells. *Biochem. Biophys. Res. Commun.* **2003**, *307*, 100–107.

(13) Wadia, J. S.; Stan, R. V.; Dowdy, S. F. Transducible TAT-HA fusogenic peptide enhances escape of TAT-fusion proteins after lipid raft macropinocytosis. *Nat. Med.* **2004**, *10*, 310–315.

(14) Rothbard, J. B.; Jessop, T. C.; Lewis, R. S.; Murray, B. A.; Wender, P. A. Role of membrane potential and hydrogen bonding in the mechanism of translocation of guanidinium-rich peptides into cells. *J. Am. Chem. Soc.* **2004**, *126*, 9506–9507.

(15) Lau, Y. H.; de Andrade, P.; Wu, Y.; Spring, D. R. Peptide stapling techniques based on different macrocyclisation chemistries. *Chem. Soc. Rev.* **2015**, *44*, 91–102.

(16) Felix, A. M.; Heimer, E. P.; Wang, C. T.; Lambros, T. J.; Fournier, A.; Mowles, T. F.; Maines, S.; Campbell, R. M.; Wegrzynski, B. B.; Toome, V.; Fry, D.; Madison, V. S. Synthesis, biological activity and conformational analysis of cyclic GRF analogs. *Int. J. Pept. Protein Res.* **1988**, *32*, 441–454.

(17) Shepherd, N. E.; Hoang, H. N.; Abbenante, G.; Fairlie, D. P. Single turn peptide alpha helices with exceptional stability in water. *J. Am. Chem. Soc.* **2005**, *127*, 2974–2983.

(18) Chu, Q.; Moellering, R. E.; Hilinski, G. J.; Kim, Y.-W.; Grossmann, T. N.; Yeh, J. T.-H.; Verdine, G. L. Towards understanding cell penetration by stapled peptides. *MedChemComm* **2015**, *6*, 111–119.

(19) Bird, G. H.; Mazzola, E.; Opoku-Nsiah, K.; Lammert, M. A.; Godes, M.; Neuberg, D. S.; Walensky, L. D. Biophysical determinants for cellular uptake of hydrocarbon-stapled peptide helices. *Nat. Chem. Biol.* **2016**, *12*, 845–852.

(20) Wallbrecher, R.; Chène, P.; Ruetz, S.; Stachyra, T.; Vorherr, T.; Brock, R. A critical assessment of the synthesis and biological activity of p53/Hdm2 stapled peptide inhibitors. *Br. J. Pharmacol.* **2017**, *174*, 2613–2622.

(21) Schmidt, S.; Adjobo-Hermans, M. J.; Kohze, R.; Enderle, T.; Brock, R.; Milletti, F. Identification of short hydrophobic cell-penetrating peptides for cytosolic peptide delivery by rational design. *Bioconjugate Chem.* **2017**, *28*, 382–389.

(22) Scheller, A.; Oehlke, J.; Wiesner, B.; Dathe, M.; Krause, E.; Beyermann, M.; Melzig, M.; Bienert, M. Structural requirements for cellular uptake of alpha-helical amphipathic peptides. *J. Pept. Sci.* **1999**, *5*, 185–194.

DOI: 10.1021/acs.jmedchem.7b00813
J. Med. Chem. 2017, 60, 8071–8082

(23) de Araujo, A. D.; Hoang, H. N.; Kok, W. M.; Diness, F.; Gupta, P.; Hill, T. A.; Driver, R. W.; Price, D. A.; Liras, S.; Fairlie, D. P. Comparative alpha-helicity of cyclic pentapeptides in water. *Angew. Chem., Int. Ed.* **2014**, *53*, 6965−6969.
(24) Ogris, M.; Carlisle, R. C.; Bettinger, T.; Seymour, L. W. Melittin enables efficient vesicular escape and enhanced nuclear access of nonviral gene delivery vectors. *J. Biol. Chem.* **2001**, *276*, 47550−47555.
(25) Juvvadi, P.; Vunnam, S.; Merrifield, R. B. Synthetic melittin, its enantio, retro, and retroenantio isomers, and selected chimeric analogs: their antibacterial, hemolytic, and lipid bilayer action. *J. Am. Chem. Soc.* **1996**, *118*, 8989−8997.
(26) Raghuraman, H.; Chattopadhyay, A. Melittin: a membrane-active peptide with diverse functions. *Biosci. Rep.* **2007**, *27*, 189−223.
(27) Marks, J. R.; Placone, J.; Hristova, K.; Wimley, W. C. Spontaneous membrane-translocating peptides by orthogonal high-throughput screening. *J. Am. Chem. Soc.* **2011**, *133*, 8995−9004.
(28) Lin, Y. Z.; Yao, S. Y.; Veach, R. A.; Torgerson, T. R.; Hawiger, J. Inhibition of nuclear translocation of transcription factor NF-kappa B by a synthetic peptide containing a cell membrane-permeable motif and nuclear localization sequence. *J. Biol. Chem.* **1995**, *270*, 14255−14258.
(29) Martín, I.; Teixidó, M.; Giralt, E. Design, synthesis and characterization of a new anionic cell-penetrating peptide: SAP(E). *ChemBioChem* **2011**, *12*, 896−903.
(30) Oehlke, J.; Scheller, A.; Wiesner, B.; Krause, E.; Beyermann, M.; Klauschenz, E.; Melzig, M.; Bienert, M. Cellular uptake of an alpha-helical amphipathic model peptide with the potential to deliver polar compounds into the cell interior non-endocytically. *Biochim. Biophys. Acta, Biomembr.* **1998**, *1414*, 127−139.
(31) Oehlke, J.; Scheller, A.; Janek, K.; Wiesner, B.; Krause, E.; Beyermann, M.; Bienert, M. Rapid translocation of amphipathic beta-helical and beta-sheet-forming peptides through plasma membranes of endothelial cells. In *Peptide Science: Present and Future*; Shimonishi, Y., Ed.; Springer: The Netherlands, 2002; pp 782−783.
(32) Eriksson, O. S.; Geörg, M.; Sjölinder, H.; Sillard, R.; Lindberg, S.; Langel, U.; Jonsson, A. B. Identification of cell-penetrating peptides that are bactericidal to Neisseria meningitidis and prevent inflammatory responses upon infection. *Antimicrob. Agents Chemother.* **2013**, *57*, 3704−3712.
(33) Perez-Jimenez, R.; Godoy-Ruiz, R.; Ibarra-Molero, B.; Sanchez-Ruiz, J. M. The efficiency of different salts to screen charge interactions in proteins: a Hofmeister effect. *Biophys. J.* **2004**, *86*, 2414−2429.
(34) Jelesarov, I.; Dürr, E.; Thomas, R. M.; Bosshard, H. R. Salt effects on hydrophobic interaction and charge screening in the folding of a negatively charged peptide to a coiled coil (leucine zipper). *Biochemistry* **1998**, *37*, 7539−7550.
(35) Strandberg, E.; Tiltak, D.; Ehni, S.; Wadhwani, P.; Ulrich, A. S. Lipid shape is a key factor for membrane interactions of amphipathic helical peptides. *Biochim. Biophys. Acta, Biomembr.* **2012**, *1818*, 1764−1776.
(36) Provencher, S. W.; Glöckner, J. Estimation of globular protein secondary structure from circular dichroism. *Biochemistry* **1981**, *20*, 33−37.
(37) van Stokkum, I. H.; Spoelder, H. J.; Bloemendal, M.; van Grondelle, R.; Groen, F. C. Estimation of protein secondary structure and error analysis from circular dichroism spectra. *Anal. Biochem.* **1990**, *191*, 110−118.
(38) Sreerama, N.; Woody, R. W. Estimation of protein secondary structure from circular dichroism spectra: comparison of CONTIN, SELCON, and CDSSTR methods with an expanded reference set. *Anal. Biochem.* **2000**, *287*, 252−260.
(39) Lobley, A.; Whitmore, L.; Wallace, B. A. DICHROWEB: an interactive website for the analysis of protein secondary structure from circular dichroism spectra. *Bioinformatics* **2002**, *18*, 211−212.
(40) Whitmore, L.; Wallace, B. A. DICHROWEB, an online server for protein secondary structure analyses from circular dichroism spectroscopic data. *Nucleic Acids Res.* **2004**, *32*, W668−73.
(41) Whitmore, L.; Wallace, B. A. Protein secondary structure analyses from circular dichroism spectroscopy: methods and reference databases. *Biopolymers* **2008**, *89*, 392−400.
(42) Wiegand, I.; Hilpert, K.; Hancock, R. E. Agar and broth dilution methods to determine the minimal inhibitory concentration (MIC) of antimicrobial substances. *Nat. Protoc.* **2008**, *3*, 163−175.
(43) Walensky, L. D.; Bird, G. H. Hydrocarbon-stapled peptides: principles, practice, and progress. *J. Med. Chem.* **2014**, *57*, 6275−6288.
(44) Bird, G. H.; Gavathiotis, E.; LaBelle, J. L.; Katz, S. G.; Walensky, L. D. Distinct BimBH3 (BimSAHB) stapled peptides for structural and cellular studies. *ACS Chem. Biol.* **2014**, *9*, 831−837.
(45) Kim, Y. W.; Verdine, G. L. Stereochemical effects of all-hydrocarbon tethers in i,i+4 stapled peptides. *Bioorg. Med. Chem. Lett.* **2009**, *19*, 2533−2536.
(46) Lättig-Tünnemann, G.; Prinz, M.; Hoffmann, D.; Behlke, J.; Palm-Apergi, C.; Morano, I.; Herce, H. D.; Cardoso, M. C. Backbone rigidity and static presentation of guanidinium groups increases cellular uptake of arginine-rich cell-penetrating peptides. *Nat. Commun.* **2011**, *2*, 453.
(47) Eiriksdottir, E.; Konate, K.; Langel, U.; Divita, G.; Deshayes, S. Secondary structure of cell-penetrating peptides controls membrane interaction and insertion. *Biochim. Biophys. Acta, Biomembr.* **2010**, *1798*, 1119−1128.
(48) Tchoumi Neree, A.; Nguyen, P. T.; Chatenet, D.; Fournier, A.; Bourgault, S. Secondary conformational conversion is involved in glycosaminoglycans-mediated cellular uptake of the cationic cell-penetrating peptide PACAP. *FEBS Lett.* **2014**, *588*, 4590−4596.
(49) Bürck, J.; Roth, S.; Windisch, D.; Wadhwani, P.; Moss, D.; Ulrich, A. S. UV-CD12: synchrotron radiation circular dichroism beamline at ANKA. *J. Synchrotron Radiat.* **2015**, *22*, 844−852.
(50) Wien, F.; Wallace, B. A. Calcium fluoride micro cells for synchrotron radiation circular dichroism spectroscopy. *Appl. Spectrosc.* **2005**, *59*, 1109−1113.
(51) Ellens, H.; Bentz, J.; Szoka, F. C. pH-induced destabilization of phosphatidylethanolamine-containing liposomes: role of bilayer contact. *Biochemistry* **1984**, *23*, 1532−1538.
(52) Berditsch, M.; Lux, H.; Babii, O.; Afonin, S.; Ulrich, A. S. Therapeutic potential of Gramicidin S in the treatment of root canal infections. *Pharmaceuticals* **2016**, *9*, 56.

DOI: 10.1021/acs.jmedchem.7b00813
J. Med. Chem. 2017, 60, 8071−8082

SUPPORTING INFORMATION

Lactam-Stapled Cell-Penetrating Peptides:

Cell Uptake and Membrane Binding Properties

Marco J. Klein[¶], Samuel Schmidt[§], Parvesh Wadhwani[¶], Jochen Bürck[¶], Johannes Reichert[¶], Sergii Afonin[¶], Marina Berditsch[#], Tim Schober[#], Roland Brock[§], Manfred Kansy[Θ] and Anne S. Ulrich[,¶#]*

[¶]Institute of Biological Interfaces (IBG-2), Karlsruhe Institute of Technology (KIT), POB 3640, 76021 Karlsruhe, Germany

[#]Institute of Organic Chemistry, KIT, Fritz-Haber-Weg 6, 76131 Karlsruhe, Germany

[§]Department of Biochemistry, Radboud Institute for Molecular Life Sciences, Radboud University Medical Center, Geert Grooteplein 28, 6525 GA Nijmegen, The Netherlands

[Θ]Roche Pharma Research and Early Development, Pharmaceutical Sciences, Roche Innovation Center Basel, F. Hoffmann-La Roche AG, Grenzacherstrasse 124, CH-4070 Basel, Switzerland

CONTENT

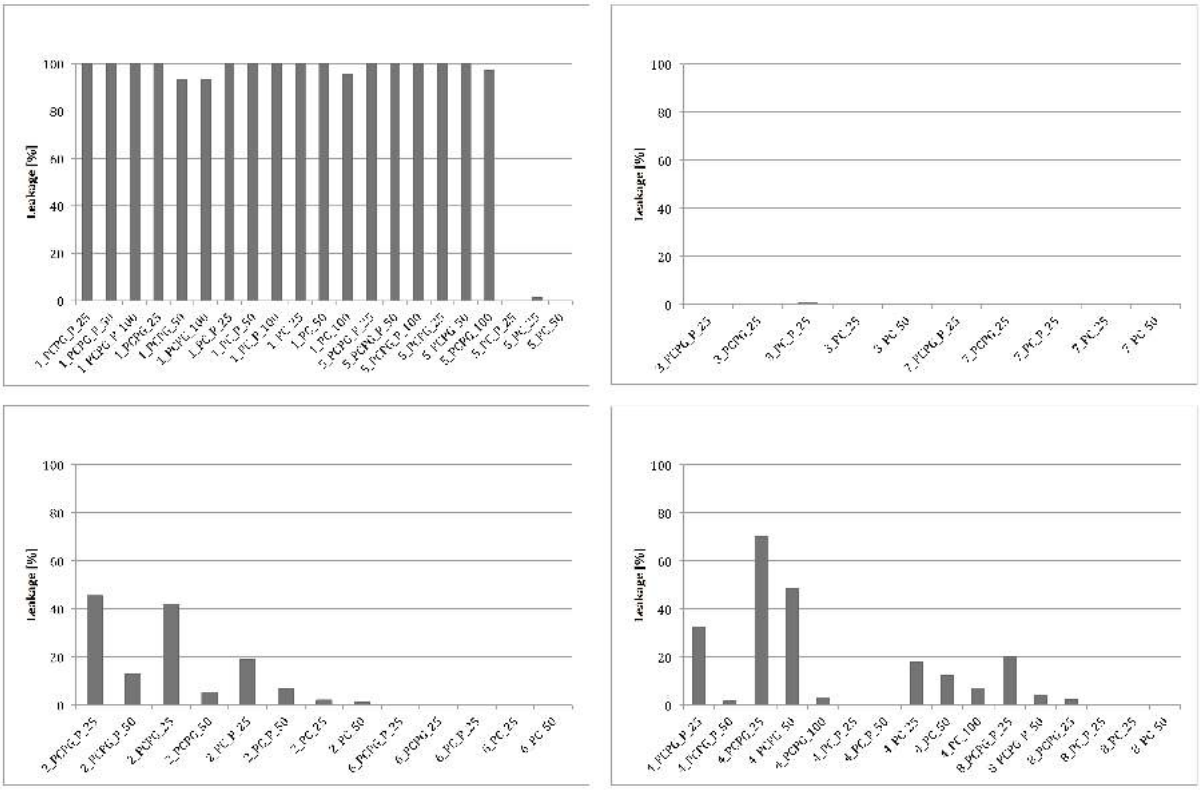

Supplemental Figure S1. Disruption of lipid vesicles consisting of POPC (PC), and POPC/POPG (PCPG) induced by the linear CPPs **1**, **2**, **3** and **4**, and their stapled analogues **5**, **6**, **7** and **8**. Vesicles were incubated with the peptides at a peptide-to-lipid ratio of 1:25 and selectively at a peptide-to-lipid ratio of 1:50 and 1:100 (when strong disruption occurred at high peptide concentrations) at a temperature of 30°C, without and with an applied membrane potential of -120 mV (P) for 30 min. The amount of lipid was kept constant for all samples. Disruption is expressed in percent of 100 % leakage induced by TritonX-100.